Icarus 288 (2017) 235–239

Contents lists available at ScienceDirect

Icarus

journal homepage: www.elsevier.com/locate/icarus

Overview of useful spectral regions for Venus: An update to encourage observations complementary to the Akatsuki mission

J. Peralta[a,*], Y.J. Lee[a], K. McGouldrick[b], H. Sagawa[c], A. Sánchez-Lavega[d], T. Imamura[e], T. Widemann[f,g], M. Nakamura[a]

[a] Institute of Space and Astronautical Science (ISAS/JAXA), Kanagawa, Japan
[b] University of Colorado, Boulder, CO, USA
[c] Faculty of Science, Kyoto Sangyo University, Japan
[d] E.T.S. Ingeniería, Universidad del País Vasco (UPV/EHU), Spain
[e] Graduate School of Frontier Sciences, University of Tokyo, Japan
[f] LESIA, Observatoire de Paris, CNRS, UPMC, Université Paris-Diderot, France
[g] Université Versailles St-Quentin, DYPAC EA 2449, France

A R T I C L E I N F O

Article history:
Received 12 September 2016
Revised 16 January 2017
Accepted 26 January 2017
Available online 9 February 2017

A B S T R A C T

New tables to observe the planet Venus are presented with detailed information about the main spectral regions from 100 nm to 1 mm. The information hereby is updated thanks to the Venus Express legacy and recent ground-based observations, and we hope it can constitute a helpful tool for professional and amateur observers willing to support and coordinate with the JAXA's Venus Climate Orbiter/Akatsuki mission.

1. Introduction

The planet Venus is permanently shrouded by a thick layer of clouds that appears featureless in the visible range. During about two centuries, attempts were made at describing the surface of Venus or measuring motions presumably apparent on its disk (Bianchini et al., 1996), but it was not until the beginning of the XXth century when a first useful narrow spectral band was found in ultraviolet, revealing global-scale dark features moving with a period of 4 days (Ross, 1928; Boyer & Camichel, 1961). During the following decades, new ranges for broadband photometry were discovered and allowed ground-based images and spectra to identify compounds of the atmosphere and clouds, characterize and constrain the atmospheric chemistry, observe the cloud morphology and winds at multiple vertical levels, estimate the temperatures at the surface and several altitudes of the atmosphere, or mapping the surface and measure the slow rotation of Venus' solid-globe (Taylor, 2014). During 2006–2014, ESA's orbiter Venus Express performed a complete characterization of the Venus atmosphere, and some new narrow spectral bands were discovered with VIRTIS (Wilson et al., 2009).

High-quality data able to overcome the worse spatial resolution in ground-based observations is possible nowadays provided the outstanding improvement in instrumentation for telescopes, along with the revolution of low-cost cameras and "lucky imaging" within the amateur community (Mousis et al. 2014). Complementary ground based observations such as these are expected to cover time and spatial gaps in observations by JAXA's Akatsuki orbiter (Nakamura et al., 2007), which has been performing regular acquisition of images to study the atmospheric dynamics of Venus since its successful orbit insertion in December 2015. Ground based observations can also extend the spectral coverage of Venus' observations during the Akatsuki mission.

2. The spectral bands to observe Venus

Tables 1 and 2 are a summary of most of the spectral bands relevant to study the Venus day side and/or night one, covering from far-ultraviolet (FUV) to microwave wavelengths. Multiple vertical levels of the Venus atmosphere can be sensed through three basic mechanisms: reflection/absorption of the sunlight on the day side, fluorescence processes and thermal emission partially absorbed by atmospheric compounds and clouds above the emitting

* Corresponding author.
E-mail address: javier.peralta@ac.jaxa.jp (J. Peralta).

http://dx.doi.org/10.1016/j.icarus.2017.01.027

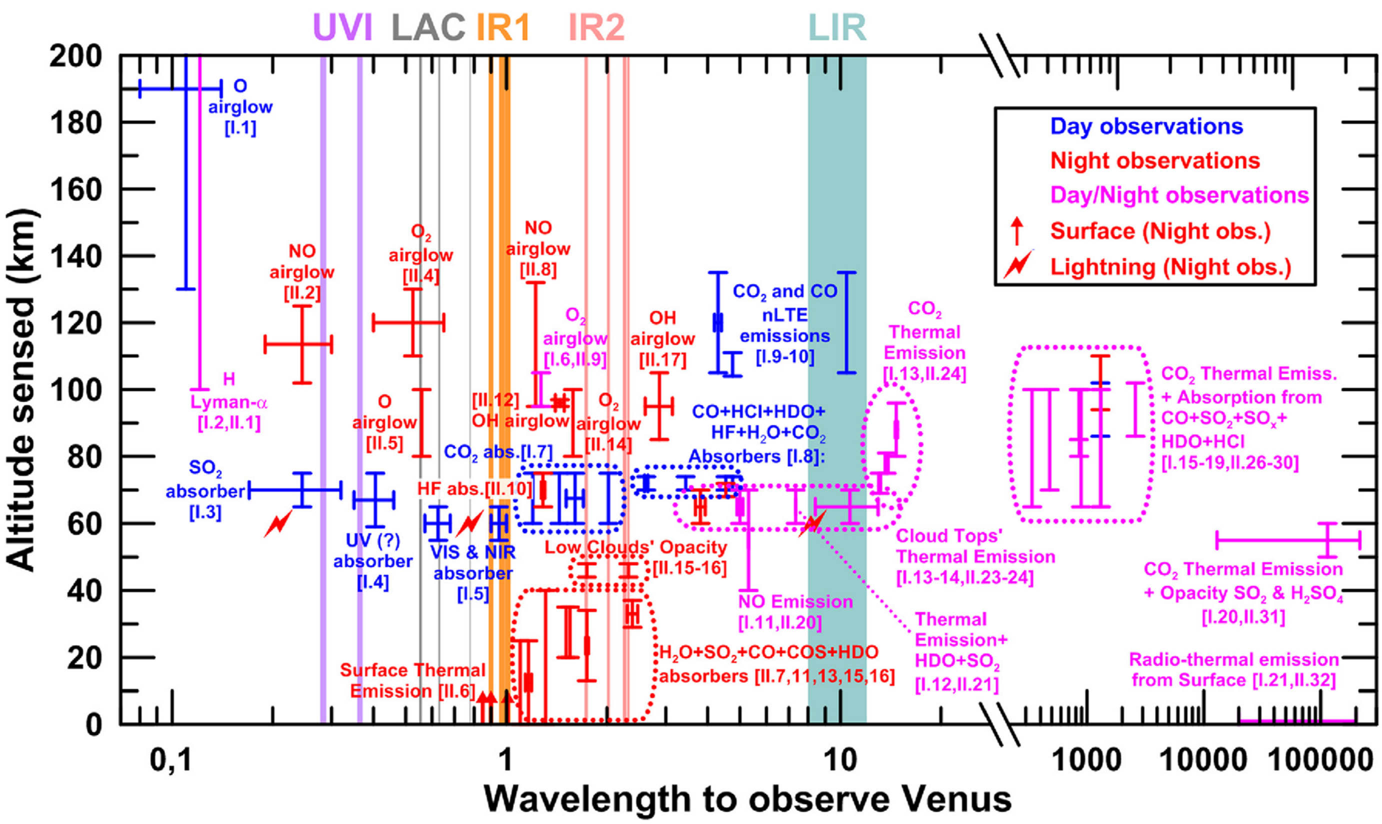

Fig. 1. Venus' spectral bands in the framework of Akatsuki's payload. References are specified in square brackets (e.g. I.19,II.30 stands for row 19 in Table 1 and row 30 in Table 2, respectively.).

layer. These processes can act simultaneously, complicating the observations; for example, the 1.27 µm O_2 nightglow emission line lies very near to the 1.31 µm spectral transparency window visible in night side thermal emission. Bands present in both tables correspond to those that can be used to sense both the day and night of Venus. The types of possible spectroscopic and imaging observations are also specified, as well as the physical parameters that can be inferred (dynamics, composition, thermal structure…) and a constraint for their inferred vertical distribution. Introductory references are also provided, with priority for detailed reviews, ground-based studies, and/or most recent measurements (including spacecraft). Fig. 1 displays most of the information from Tables 1 and 2 in the framework of the spectral coverage Akatsuki's cameras (Nakamura et al., 2007). Even though the atmospheric transmission on the Earth severely limits the observations at certain spectral ranges, these limitations can be partially overcome by airborne observations, balloons and space telescopes, and also using sophisticated radiative transfer models able to remove from the Venus spectra blended with lines originated by the terrestrial atmosphere (Cotton et al., 2012).

Table 1 displays the relevant bands when observing the day side of Venus, doubtless the easiest target for amateur observers since ultraviolet (UV), visible (VIS) and near-infrared (NIR) commercial filters allow to perform wind measurements with feature tracking at the upper clouds (Mousis et al. 2014). Some IR CO_2 bands can be also used on the day side to infer the altitude of the cloud tops (Ignatiev et al., 2009), and valuable observations can be done with the new generation of high-resolution spectrometers, from measuring Doppler winds (Machado et al., 2012) to studying the sulphur cycle (Marcq et al., 2011), the unknown UV absorber whose absorption might extend beyond the band in Table 1 (Tomasko et al., 1980; Marcq et al., 2011), or the thermal structure and complex atmospheric circulation of the upper atmosphere with the non-LTE emissions (Sornig et al., 2008; Peralta et al., 2016). Unfortunately, observations at FUV –which allow to study the ion population and circulation in the Venus' thermosphere– and at some infrared ranges are impossible from the ground because of Earth's low atmospheric transmittance; alternatively, airborne or satellite observations should be used (Bougher et al., 2006).

Table 2 exhibits the wavelengths useful to sense the night side of Venus. These are dominated by bands in the infrared range usually demanding longer exposures and more sensitive cameras, although amateur observers have observed the thermal emission from the Venus surface and atmosphere using NIR filters (Mousis et al. 2014). In addition to several types of nightglow occurring above the cloud tops at UV and VIS wavelengths (Gray et al., 2014), some critical CO_2 bands can be utilized to derive the atmospheric temperature at multiple levels (Grassi et al., 2008) or the altitude of the cloud tops (Ignatiev et al., 2009). Of great relevance is the IR interval 2.30–2.47 µm, which allow to derive multiple compounds from the deep atmosphere below the clouds (Arney et al., 2014). IR wavelengths at 1.74 µm and 2.32 µm can be also used to sense the motions of the lower clouds (Limaye et al., 2006; Sánchez-Lavega et al., 2008). Since the clouds of Venus can potentially generate lightning, predicted bands to observe them are also included (Dubrovin et al., 2010; Pérez-Invernón et al., 2016). Although out of the range of our study, we would like to mention that X-ray observations have also been reported on the nightside of Venus (Dennerl et al., 2002; Afshari et al., 2016).

Table 1
Venus's spectral bands for day side observations. Wavelength ranging from FUV to microwave are expressed in nanometres (nm), micrometres (μm) and Gigahertz (GHz) depending on the spectral region, and these are followed by an asterisk (e.g. μm*) when the band can be used for the same purpose in both day and night sides of Venus. The technique can be imaging (IMAG) or spectroscopy (SPEC), while the products are the parameters that can be derived are gas abundances (e.g. [CO_2]), atmospheric temperature (Temp), aerosols' properties and distribution (Aer), winds and waves from feature tracking (Track), winds from the Doppler technique (Doppler), and surface studies (mapping, temperature, composition and geological processes) are expressed as Surf. The vertical range sensed, processes involved in the emerging radiance and References are also specified.

Wavelength	Products	Altitude	Processes	References
80–140 nm (esp. 83.4, 130,4, 135.6, 130.4, 135.6)	SPEC: [OI], [OII], [O/CO_2], Temp, Doppler?	130–250 km	O airglow	Bougher et al. (2006), Hubert et al. (2010), Masunaga et al. (2015)
121 nm*	SPEC: [H], [D/H]	100–8000 km	Hydrogen Lyman-α emission	Chaufray et al. (2015), Bertaux (1989)
170–320 nm	SPEC: [SO_2], Aer IMAG: Track	> 70 km	SO_2 absorption + sunlight reflected by clouds	Jessup et al. (2015)
350–460 nm (max. contrast at 360–370 nm)	SPEC: [UV absorber], Doppler, Aer IMAG: Track, Aer	63–71 km	UV absorption + sunlight reflected by clouds	Tomasko et al. (1980), Sánchez-Lavega et al. (2008), Mousis (2014)
570–680 & 900–1000 nm	SPEC: Aer, Doppler IMAG: Track, Aer	55–65 km	VIS & NIR sunlight reflected by clouds	Sánchez-Lavega et al. (2008), Mousis (2014), Hueso et al. (2015), Takagi and Iwagami (2011)
1.27 μm	SPEC: [O] IMAG: [O], Track	~ 95 km	O_2 airglow	Connes et al. (1979)
1.20, 1.44, 1.51–1.70, 2.02 μm	SPEC/IMAG: Altitude of clouds' top, Track	60–75 km	CO_2 absorption	Ignatiev et al. (2009), Takagi and Iwagami (2011)
2.59–2.65, 3.44, 4.53, 4.75 μm	SPEC: [H_2O], [HDO], [HF], [CO_2], [HCl], [CO], Temp	70–74 km	Absorption by several species & isotopologues	Bjoraker et al. (1992), Krasnopolsky (2010, 2014), Marcq et al. (2015)
4.20–4.40 μm 10.423 μm	SPEC: Temp, Doppler IMAG: Track	105–135 km	CO_2 nLTE emission	Peralta et al. (2016), Sornig et al. (2008)
4.75 μm	SPEC: [CO], Temp.	104–111 km	CO nLTE emission	Krasnopolsky (2014)
5.3 μm*	SPEC: [NO]	From 100 km to below 50 km	NO rotational-band emission	Krasnopolsky (2006)
7.35 μm*	SPEC: [HDO], [SO_2], Temp	60–70 km	Thermal emission + sunlight reflected by cloud tops + emission HDO + SO_2	Encrenaz et al. (2012)
5.00–… μm* 8.40–12.96 μm*	SPEC: Temp IMAG: Temp, Track	60–70 km	Thermal emission + sunlight reflected by cloud tops	García-Muñoz et al. (2013), Sato (2014), Takagi and Iwagami (2011)
13.0–13.2 μm* 13.6–13.9 μm* 14.6–14.8 μm*	SPEC: Temp IMAG: Temp, Track	69–75 km 75–81 km 80–96 km	CO_2 thermal emission	Taylor et al. (1980)
893, 335, 226 GHz*	SPEC: [HDO]	65–100 km	HDO absorption	Encrenaz et al. (2015), Sandor (2005), Hartogh et al. (2014)
625 GHz*	SPEC: [HCl]	70–100 km	HCl absorption	Sandor (2012), Hartogh et al. (2014)
115, 230, 345 GHz*	SPEC: [CO], Doppler, Temp	90–110 km (different for day & night)	CO absorption	Lellouch et al. (2008), Clancy et al. (2012)
352.8 GHz*	SPEC: [ClO]	>85 km	ClO absorption	Sandor (2013)
346.6 GHz*	SPEC: [SO], [SO_2]	~80–100 km	SOx absorption	Encrenaz et al. (2015)
23–1.385 GHz*	SPEC: [SO_2], [H_2SO_4], Temp	50–60 km	Thermal emission CO_2 CIA (main) with opacity by SO_2 & H_2SO_4	Butler et al. (2001), Jenkins et al. (2002)
15–1.50 GHz*	IMAG: Surf	Surface	Surface Radio-Thermal emission	Campbell et al. (2015)

Finally, both Tables exhibit at longer wavelengths several common bands of special interest, since they allow to visualize the day and night of Venus simultaneously and at similar heights, except for concrete exceptions like the CO (Lellouch et al., 2008). Mid-infrared bands sense the thermal emission from the upper clouds to about 90 km (Taylor et al. 1980; García-Muñoz et al., 2013), while sub-millimetre and microwave heterodyne observations can cover a wider vertical range in the upper atmosphere and allow to sense the rotational transitions of mesospheric minor species such as CO, HDO, SO, SO_2, and HCl (Encrenaz et al., 2015). CO lines are used to sense the atmospheric temperature and Doppler winds using sub-millimetre heterodyne spectroscopy (Lellouch et al., 2008; Clancy et al., 2012). At longer wavelengths in microwave, we can sense the atmosphere below the clouds since the CO_2 collision-induced absorption becomes weaker (Jenkins et al., 2002). Lightning was indirectly detected via whistler waves at 1–10 Hz by Venus Express (Russell et al., 2007), and it has been also proposed that it might be detected at 5–50 MHz using UHF detectors in a low Venus orbit (Majid et al., 2013). At further long wavelengths in radar domain (~2.3 GHz, 12.6 cm), the atmosphere of Venus becomes quite transparent and the surface can be imaged (Campbell et al., 2015), while subsurface sounding has been also suggested to be possible at the 10–30 MHz range (Biccari et al., 2004).

Acknowledgements

JP acknowledges JAXA's International Top Young Fellowship. A.S.-L. was supported by the Spanish project AYA2015-65041-P (MINECO/FEDER), Grupos Gobierno Vasco IT-765-13 and Universidad del País Vasco UPV/EHU program UFI11/55. All the authors acknowledge support from the Akatsuki Project. This work is based in an original idea by D. Fischer to motivate ground-based observations during ESA's Venus Express mission.

Table 2
Venus's spectral bands for night side observations. Information and notation is the same as in Table 1.

Wavelength	Products	Altitude	Processes	References
121 nm*	SPEC: [H], [D/H]	100–10,000 km	Hydrogen Lyman-α emission	Chaufray et al. (2015), Bertaux (1989)
190–300 nm	SPEC: [N], [O]	102–125 km	NO nightglow	Krasnopolsky (2006)
120–280, 208, 250–450 nm	IMAG: lightning?	Cloud region or above?	Electric discharge in N_2–CO_2 mixture	Dubrovin et al. (2010), Pérez-Invernón et al. (2016)
400–650 nm	SPEC: [O_2] IMAG: Track	100–130 km	Herzberg II O_2 nightglow	García-Muñoz et al. (2009b)
557.7 & 777.3 nm	SPEC: [O] IMAG: lightning?	Upper atmosphere	O nightglow & aurora & electric discharge in N_2–CO_2 mixture	Gray et al. (2014), Dubrovin et al. (2010), Pérez-Invernón et al. (2016)
850 & 900 nm 1.01 µm	IMAG: Surf	Surface (main source)	Surf. thermal emission + clouds' opacity	Baines (2000), Mousis (2014)
1.14–1.19, 1.10 µm	IMAG: Surf, [H_2O], [HDO]	0–25 km	Surf. thermal emission + Abs. HDO+H_2O	Bailey et al. (2008b), Bézard et al. (2011)
1.224 µm	SPEC: [NO]	95 – 132 km	NO nightglow	García-Muñoz et al. (2009a)
1.269 µm	SPEC/IMAG: [O], Temp, Track	95–105 km	O_2 airglow from O recombination	Ohtsuki et al. (2008), Bailey et al. (2008a),
1.273–1.304 µm	SPEC: [HF]	Cloud tops	HF absorption	Connes et al. (1967), Krasnopolsky (2010)
1.31 µm	SPEC: ? IMAG: Track?	Between clouds and surface	Scattering of surface thermal emission, weak	Mueller et al. (2008)
1.40–1.49 µm	SPEC: [OH]	∼ 96 km	OH nightglow	Piccioni et al. (2008)
1.51 & 1.55 µm	SPEC: [H_2O] IMAG: [H_2O]	20–35 km	Unexplained minimum in H_2O absorption	Wilson et al. (2009)
1.58 µm	SPEC/IMAG: [O], Temp?	Upper atmosphere	O_2 airglow	Bailey et al. (2008b)
1.727–1.758 µm	SPEC: [HCl], [H_2O] IMAG: Track	Species: 13–34 km Clouds: 44–48 km	Absorption by several species + Thermal Emission + Clouds opacity	Sánchez-Lavega et al. (2008), Bézard (2007), Arney et al. (2014)
2.30–2.47 µm	SPEC: [CO], [HDO], [H_2O], [OCS], [SO_2] IMAG: Track	Species: 26–40 km Clouds: 44–48 km	Absorption by several species + Thermal Emission + Clouds opacity	Limaye et al. (2006), Bézard (2007), Arney et al. (2014), Takagi and Iwagami (2011)
2.60–3.14 (2.80 & 2.94)	SPEC: [OH]	95 ± 10 km	OH nightglow	Piccioni et al. (2008)
4.25–5.00	SPEC: Temp	50–100 km	CO_2 emission	Grassi et al. (2008)
4.53 µm	SPEC: [CO]	∼ 70 km	CO absorption	Marcq et al. (2015)
5.3 µm*	SPEC: [NO]	From 100 km to below 50 km	NO rotational-band emission	Krasnopolsky (2006)
7.35 µm*	SPEC: [HDO], [SO_2], Temp	60–70 km	Thermal emission from upper clouds + emission HDO + SO_2	Encrenaz et al. (2012)
8.25 µm	IMAG: lightning?	Cloud region or above?	Electric discharge in N_2–CO_2 mixture	Pérez-Invernón et al. (2016)
3.68–3.94 µm 4.81–4.89 µm 5.00–... µm* 8.40–13.0 µm*	SPEC: Temp IMAG: Temp, Track	60–70 km	Thermal emission from upper clouds	Taylor et al. (1980), Sato (2014), García-Muñoz et al. (2013), Takagi and Iwagami (2011)
13.0–13.2 µm* 13.6–13.9 µm* 14.6–14.8 µm*	SPEC: Temp IMAG: Temp, Track	69–75 km 75–81 km 80–96 km	CO_2 thermal emission	Taylor et al. (1980)
136.1 µm	IMAG: lightning?	Cloud region or above?	Electric discharge in N_2–CO_2 mixture	Pérez-Invernón et al. (2016)
893, 335, 226 GHz*	SPEC: [HDO]	65–100 km	HDO absorption	Encrenaz et al. (2015), Sandor (2005), Hartogh et al. (2014)
625 GHz*	SPEC: [HCl]	70–100 km	HCl absorption	Sandor (2012), Hartogh et al. (2014)
115, 230, 345 GHz*	SPEC: [CO], Doppler, Temp	90–110 km (different for day & night)	CO absorption	Lellouch et al. (2008), Clancy et al. (2012)
352.8 GHz*	SPEC: [ClO]	> 85 km	ClO absorption	Sandor (2013)
346.6 GHz*	SPEC: [SO], [SO_2]	∼80–100 km	SOxabsorption	Encrenaz et al. (2015)
23–1.385 GHz*	SPEC: [SO_2], [H_2SO_4], Temp	50–60 km	Thermal emission CO_2 CIA (main) with opacity by SO_2& H_2SO_4	Butler et al. (2001), Jenkins et al. (2002)
15–1.50 GHz*	IMAG: Surf	Surface	Surface Radio-Thermal emission	Campbell et al. (2015)

References

Afshari, M., Peres, G., Jibben, P.R., Petralia, A., et al., 2016. X-raying the dark side of Venus–Scatter from Venus' Magnetotail. Astron. J. 152 (4).

Arney, G., Meadows, V., Crisp, D., et al., 2014. Spatially resolved measurements of H_2O, HCl, CO, OCS, SO_2, cloud opacity, and acid concentration in the Venus near-infrared spectral windows. J. Geophys. Res. Planets 119, 1860–1891.

Baines, K.H.and 24 colleagues, 2000. Detection of sub-micron radiation from the surface of Venus by Cassini/VIMS. Icarus 148, 307–311.

Bailey, J., Meadows, V.S., Chamberlain, S., Crisp, D., 2008a. The temperature of the Venus mesosphere from O_2 ($a^1\Delta_g$) airglow observations. Icarus 197, 247–259.

Bailey, J., Chamberlain, S., Crisp, D., et al., 2008. Near infrared imaging spectroscopy of Venus with the Anglo-Australian telescope. Planet. Space Sci. 56, 1385–1390.

Bertaux, J.-L., Clarke, J.T., 1989. Deuterium content of the Venus atmosphere. Nature 338, 567–568.

Bézard, B., de Bergh, C., 2007. Composition of the atmosphere of Venus below the clouds. J. Geophys. Res. 112, E04S07.

Bézard, B., Fedorova, A., Bertaux, J.-L., et al., 2011. The 1.10 and 1.18 µm nightside windows of Venus observed by SPICAV-IR aboard Venus express. Icarus 216, 173–183.

Bianchini, F., Beaumont, S., Fay, P., 1996. Observations Concerning the Planet Venus. Springer-Verlag Berlin Heidelberg, New York, p. 172.

Biccari, D., Calabrese, D., Gurnett, D., Huff, R., et al., 2004. VENUS subsurface ionosphere radar sounder: VENSIS. In: 3DPVT Proceedings. IEEE, 2004, pp. 931–937.

Bjoraker, G.L., Larson, H.P., Mumma, M.J., et al., 1992. Airborne observations of the gas composition of Venus above the cloud tops: Measurements of H_2O, HDO, HF and the D/H and $^{18}O/^{16}O$ isotope ratios. Bull. Am. Astron. Soc. 24, 995 (1992).

Bougher, S.W., Rafkin, S., Drossart, P., 2006. Dynamics of the Venus upper atmosphere: outstanding problems and new constraints expected from Venus express. Planet. Space Sci. 54, 1371–1380.

Boyer, C., Camichel, H., 1961. Observations photographiques de la planète Vénus. Annales d'Astrophysique 24, 531–535.

Butler, B.J., Steffes, P.G., Suleiman, S.H., et al., 2001. Accurate and consistent microwave observations of Venus and their implications. Icarus 154, 226–238.

Campbell, B.A., Campbell, D.B., Morgan, G.A., et al., 2015. Evidence for crater ejecta on Venus tessera terrain from Earth-based radar images. Icarus 250, 123–130.

Chaufray, J.-Y., Bertaux, J.-L., Quémerais, E., et al., 2015. Observations of the nightside venusian hydrogen corona with SPICAV/VEX. Icarus 262, 1–8.

Clancy, R.T., Sandor, B.J., Moriarty-Schieven, G., 2012. Circulation of the Venus upper mesosphere/lower thermosphere. Icarus 217, 794–812.

Connes, P., Connes, J., Benedict, W.S., Kaplan, L.D., 1967. Traces of HCl and HF in the atmosphere of Venus. ApJ 147, 1230–1237.

Connes, P., Noxon, J.F., Traub, W.A., et al., 1979. $O_2(^1\Delta)$ emission in the day and night airglow of Venus. ApJ 233, L29–L32.

Cotton, D.V., Bailey, J., Crisp, D., Meadows, V.S., 2012. The distribution of carbon monoxide in the lower atmosphere of Venus. Icarus 217, 570–584.

Dennerl, K., Burtwitz, V., Englhauser, J., Lisse, C., Wolk, S., 2002. Discovery of X-rays from Venus with Chandra. A&A 386, 319–330.

Dubrovin, D., Nijdam, S., van Veldhuizen, E.M., et al., 2010. Sprite discharges on Venus and Jupiter-like planets: a laboratory investigation. J. Geophys. Res. 115, A00E34.

Encrenaz, T., Greathouse, T.K., Roe, H., et al., 2012. HDO and SO_2 thermal mapping on Venus: evidence for strong SO_2 variability. A&A 543 (7), idA153.

Encrenaz, T., Moreno, R., Moullet, A., et al., 2015. Submillimeter mapping of mesospheric minor species on Venus with ALMA. Planet. Space Sci. 113, 275–291.

García-Muñoz, A., Mills, F.P., Piccioni, G., et al., 2009a. The near-infrared nitric oxide nightglow in the upper atmosphere of Venus. Proc. Nat. Acad. Sci. 106, 985–988.

García-Muñoz, A., Mills, F.P., Slanger, T.G., et al., 2009b. Visible and near-infrared nightglow of molecular oxygen in the atmosphere of Venus. J. Geophys. Res. 114, E12002.

García-Muñoz, A., Wolkenberg, P., Sánchez-Lavega, A., et al., 2013. A model of scattered thermal radiation for Venus from 3 to 5 µm. Planet. Space Sci. 81, 6573.

Grassi, D., Drossart, P., Piccioni, G., et al., 2008. Retrieval of air temperature profiles in the Venusian mesosphere from VIRTIS-M data. J. Geophy. Res. 113, E00B09.

Gray, C.L., Chanover, N.J., Slanger, T.G., et al., 2014. The effect of solar flares, coronal mass ejections, and solar wind streams on Venus' 5577 Å oxygen green line. Icarus 233, 342–347.

Hartogh, P., Sagawa, H., Rengel, M., 2014. APEX submillimeter observations of HCl and HDO in the mesosphere of Venus, 2014. COSPAR Meeting, 40, B0.7–10-14.

Hueso, R., Peralta, J., Garate-Lopez, I., et al., 2015. Six years of Venus winds at the upper cloud level from UV, visible and near infrared observations from VIRTIS on Venus express. Planet. Space Sci. 113-114, 78–99.

Hubert, B., Gérard, J.C., Gustin, J., et al., 2010. UVIS observations of the FUV OI and CO 4P Venus dayglow during the Cassini flyby. Icarus 207, 549–557.

Ignatiev, N.I., Titov, D.V., Piccioni, G., et al., 2009. Altimetry of the Venus cloud tops from the Venus Express observations. J. Geophys. Res. 114, E00B43.

Jenkins, J.M., Kolodner, M.A., Butler, B.J., et al., 2002. Microwave remote sensing of the temperature and distribution of sulfur compounds in the lower atmosphere of Venus. Icarus 158, 312–328.

Jessup, K.L., Marcq, E., Mills, F., et al., 2015. Coordinated hubble space telescope and Venus express observations of Venus' upper cloud deck. Icarus 258, 309–336.

Krasnopolsky, V.A., 2006. A sensitive search for nitric oxide in the lower atmospheres of Venus and Mars: detection on Venus and upper limit for Mars. Icarus 182, 80–91.

Krasnopolsky, V.A., 2010. Spatially-resolved high-resolution spectroscopy of Venus 1. Variations of CO_2, CO, HF, and HCl at the cloud tops. Icarus 208, 539–547.

Krasnopolsky, V.A., 2014. Observations of CO dayglow at 4.7 µm, CO mixing ratios, and temperatures at 74 and 104-111 km on Venus. Icarus 237, 340–349.

Lellouch, E., Paubert, G., Moreno, R., Moullet, A., 2008. Monitoring Venus' mesospheric winds in support of Venus express: IRAM 30-m and APEX observations. Planet. Space Sci. 56, 1355–1367.

Limaye, S.S., Warell, J., Bhatt, B.C., et al., 2006. Multi-observatory observations of night-side of Venus at 2.3 µ - atmospheric circulation from tracking of cloud features. Bull. Astron. Soc. India 34, 189–201.

Machado, P., Luz, D., Widemann, T., et al., 2012. Mapping zonal winds at Venus's cloud tops from ground-based Doppler velocimetry. Icarus 221, 248–261.

Majid, W., Duncan, C., Kuiper, T., Russell, C.T., et al., 2013. A Cubesat Mission to Venus: a Low-Cost Approach to the Investigation of Venus lightning AGU, P41D1946.

Marcq, E., Belyaev, D., Montmessin, F., et al., 2011. An investigation of the SO_2 content of the venusian mesosphere using SPICAV-UV in nadir mode. Icarus 211, 58–69.

Marcq, E., Lellouch, E., Encrenaz, T., et al., 2015. Search for horizontal and vertical variations of CO in the day and night side lower mesosphere of Venus from CSHELL/IRTF 4.53 µm observations. Planet. Space Sci. 113, 256–263.

Masunaga, K., Seki, K., Terada, N., et al., 2015. Periodic variations of oxygen EUV dayglow in the upper atmosphere of Venus: Hisaki/EXCEED observations. J. Geophys. Res. Planets 120, 2037–2052.

Mousis, O.and 59 colleagues, 2014. Instrumental methods for professional and amateur collaborations in planetary astronomy. Exp. Astron. 38, 91–191.

Mueller, N., Helbert, J., Hashimoto, G.L., et al., 2008. Venus surface thermal emission at 1 µm in VIRTIS imaging observations: Evidence for variation of crust and mantle differentiation conditions. J. Geophys. Res. 113, E00B17.

Nakamura, M., Imamura, T., Ueno, M., et al., 2007. Planet-C: Venus climate orbiter mission of Japan. Planet. Space Sci. 55, 1831–1842.

Ohtsuki, S., Iwagami, N., Sagawa, H., et al., 2008. Imaging spectroscopy of the Venus 1.27 µm O_2 airglow with ground-based telescopes. Adv. Space Res. 41, 1375–1380.

Peralta, J., López-Valverde, M.A., Gilli, G., Piccialli, A., 2016. Dayside temperatures in the Venus upper atmosphere from Venus Express/VIRTIS nadir measurements at 4.3 µm. A&A 585, 7 id.A53.

Pérez-Invernón, F.J., Luque, A., Gordillo-Vázquez, F.J., 2016. Mesospheric optical signatures of possible lightning on Venus. J. Geophys. Res. Space Phys. 121. doi:10.1002/2016JA022886.

Piccioni, G., Drossart, P., Zasova, L., et al., 2008. First detection of hydroxyl in the atmosphere of Venus. A&A 483, L29–L33.

Ross, F.E., 1928. Photographs of Venus. ApJ 68, 57.

Russell, C.T., Zhang, T.L., Delva, M., Magnes, W., Strangeway, R.J., Wei, H.Y., 2007. Lightning on Venus inferred from whistler-mode waves in the ionospere. Nature 450, 661–662.

Sánchez-Lavega, A., Hueso, R., Piccioni, G., et al., 2008. Variable winds on Venus mapped in three dimensions. Geophys. Res. Lett. 35, L13204.

Sandor, B.J., Clancy, R.T., 2005. Water vapor variations in the Venus mesosphere from microwave spectra. Icarus 177, 129–143.

Sandor, B.J., Clancy, R.T, 2012. Observations of HCl altitude dependence and temporal variation in the 70–100 km mesosphere of Venus. Icarus 220, 618–626.

Sandor, B.J., Clancy, R., 2013. First measurements of ClO in the Venus mesosphere. AAS id202, 02 DPS meeting #45.

Sato, T.M., Sagawa, H., Kouyama, T., et al., 2014. Cloud top structure of Venus revealed by Subaru/COMICS mid-infrared images. Icarus 243, 386–399.

Sornig, M., Livengood, T., Sonnabend, G., Kroetz, P., Stupar, D., Kostiuk, T., Schieder, R., 2008. Venus upper atmosphere winds from ground-based heterodyne spectroscopy of CO_2 at 10 µm wavelength. Planet. Space Sci. 56, 1399–1406.

Takagi, S., Iwagami, N., 2011. Contrast sources for the infrared images taken by the Venus mission AKATSUKI. Earth planets space 63 (5), 435–442.

Taylor, F.W., et al., 1980. Structure and meteorology of the middle atmosphere of Venus Infrared remote sensing from the Pioneer orbiter. J. Geophys. Res. 85, 7963–8006.

Taylor, F.W., 2014. The Scientific Exploration of Venus. Cambridge Univ. Press, p. 2014.

Tomasko, M.G., Doose, L.R., Smith, P.H., et al., 1980. Measurements of the flux of sunlight in the atmosphere of Venus. J. Geophys. Res. 85, 8167–8186.

Wilson, C.F., Tsang, C.C.C., Irwin, P.G.J., et al., 2009. Analysis of thermal emission from the nightside of Venus at 1.51 and 1.55 µm. Icarus 201, 814–817.